ARTICLE

Check for updates

Cellular and Molecular Biology

PCK1 regulates neuroendocrine differentiation in a positive feedback loop of LIF/ZBTB46 signalling in castration-resistant prostate cancer

Yu-Ching Wen[1,2,3,11], Chien-Liang Liu[4,11], Hsiu-Lien Yeh[5], Wei-Hao Chen[6], Kuo-Ching Jiang[6], Van Thi Ngoc Tram[6], Michael Hsiao[7], Jiaoti Huang[8], Wei-Yu Chen[9,10]✉ and Yen-Nien Liu[6]✉

BACKGROUND: Castration-resistant prostate cancer (CRPC) patients frequently develop neuroendocrine differentiation, with high mortality and no effective treatment. However, the regulatory mechanism that connects neuroendocrine differentiation and metabolic adaptation in response to therapeutic resistance of prostate cancer remain to be unravelled.
METHODS: By unbiased cross-correlation between RNA-sequencing, database signatures, and ChIP analysis, combining in vitro cell lines and in vivo animal models, we identified that PCK1 is a pivotal regulator in therapy-induced neuroendocrine differentiation of prostate cancer through a LIF/ZBTB46-driven glucose metabolism pathway.
RESULTS: Upregulation of PCK1 supports cell proliferation and reciprocally increases ZBTB46 levels to promote the expression of neuroendocrine markers that are conducive to the development of neuroendocrine characteristic CRPC. PCK1 and neuroendocrine marker expressions are regulated by the ZBTB46 transcription factor upon activation of LIF signalling. Targeting PCK1 can reduce the neuroendocrine phenotype and decrease the growth of prostate cancer cells in vitro and in vivo.
CONCLUSION: Our study uncovers LIF/ZBTB46 signalling activation as a key mechanism for upregulating PCK1-driven glucose metabolism and neuroendocrine differentiation of CRPC, which may yield significant improvements in prostate cancer treatment after ADT using PCK1 inhibitors.

British Journal of Cancer (2022) 126:778–790; https://doi.org/10.1038/s41416-021-01631-3

BACKGROUND

Prostate cancer (PCa) is one of the most common human male malignancies and is frequently managed with androgen deprivation therapy (ADT), which initially reduces the tumour burden, but resistance still occurs, known as castration-resistant PCa (CRPC) [1]. A subset of PCa patients with ADT resistance who are treated with conventional androgen receptor (AR)-targeted therapy may progress to an androgen-independent phenotype and exhibit strong neuroendocrine (NE) characteristics, which is termed CRPC-NE [2]. The histopathological characteristics of CRPC-NE are similar to other NE tumours [3]. CRPC-NE can be classified into small-cell carcinoma (SCPC), large cell NE carcinoma, carcinoid, and adenocarcinoma with NE differentiation [4]. The incidence of CRPC-NE is increasing due to the widespread use of AR pathway inhibitors (ARPIs) and hormonal therapy, which subsequently leads to the differentiation of NE-like cells acquire cancer stem-like cell signalling, called treatment-induced NE PCa (t-NEPC) [5]. Because of the absence of therapeutic biomarkers, the prognosis of CRPC-NE patients is poor, and the overall survival of patients with CRPC-NE may be less than 2 years [2]. Therefore, an understanding of the mechanisms of CRPC-NE is urgently needed to treat the increasing numbers of PCa patients with therapeutic resistance.

CRPC development is related to metabolic reprogramming [6]. Activation of the glucose metabolism pathway in ADT-resistant PCa cells promotes ATP biosynthesis, and the upregulation of glycolytic genes increases glucose consumption and lactate production, leading to tumorigenesis [7]. Phosphoenolpyruvate (PEP) carboxykinase 1 (PCK1) is a cytosolic enzyme that catalysers the transformation of oxaloacetate (OAA) into PEP, which induces non-carbohydrate sources to enter glycolysis and acts as a pivotal regulator of low-nutrient adaptation [8]. The catalytic efficiency of

[1]Department of Urology, Wan Fang Hospital, Taipei Medical University, Taipei, Taiwan. [2]Department of Urology, School of Medicine, College of Medicine, Taipei Medical University, Taipei, Taiwan. [3]TMU Research Center of Urology and Kidney, Taipei medical university, Taipei, Taiwan. [4]Division of Urology, Department of Surgery, Chi Mei Medical Center, Tainan, Taiwan. [5]General Education Development Center, Hsin Sheng Junior College of Medical Care and Management, Taoyuan, Taiwan. [6]Graduate Institute of Cancer Biology and Drug Discovery, College of Medical Science and Technology, Taipei Medical University, Taipei, Taiwan. [7]Genomics Research Center, Academia Sinica, Taipei, Taiwan. [8]Department of Pathology, Duke University Medical Center, Durham, NC, USA. [9]Department of Pathology, Wan Fang Hospital, Taipei Medical University, Taipei, Taiwan. [10]Department of Pathology, School of Medicine, College of Medicine, Taipei Medical University, Taipei, Taiwan. [11]These authors contributed equally: Yu-Ching Wen, Chien-Liang Liu. ✉email: 1047@tmu.edu.tw; liuy@tmu.edu.tw

Received: 5 August 2021 Revised: 24 October 2021 Accepted: 3 November 2021
Published online: 24 November 2021

PCK1 depends on the surrounding glucose concentration; as the surrounding glucose concentration decreases, the catalytic capacity of PCK1 increases [9]. Although PCK1 is one of the key regulators of metabolic reprogramming supporting energy production [8], the expression of PCK1 is positively correlated with tumour progression and metastasis of gastric cancer [10] and colorectal cancer (CRC) [11, 12]. An elevated level of PCK1 promotes the tricarboxylic acid (TCA) cycle and activates the RAS/ extracellular signal-regulated kinase (ERK) signalling pathway to induce matrix metalloprotease (MMP)-9 expression, finally triggering gastric cancer metastasis [10]. An increase in PCK1 promotes cancer cell growth by improving glucose and glutamine utilisation, and induces pyrimidine synthesis for hepatic metastasis in CRC [11, 12]. Nevertheless, PCK1 may also function as a tumour suppressor in hepatocellular carcinoma (HCC), in which its deficiency promotes cell proliferation by inducing oxidative stress and activation of the transcription factor nuclear factor, erythroid 2 like 2 (NRF2) [13]. In PCa, the increase in PCK1 levels may be associated with the enhancement of PCa development by normal prostate-derived stromal cells, but the mechanism is unknown [14]. As ADT is known to be associated with metabolic disorders in PCa [15], the mechanism of upregulation of PCK1 with a significantly increased risk of glucose metabolism pathway disorders and the malignant progression of ADT-resistant PCa remains unidentified.

Based on results from our previous study, the leukaemia-inhibitory factor (LIF)/zinc finger and BTB domain-containing 46 (ZBTB46) axis is activated in PCa tumours after ADT and contributes to therapeutic resistance and lineage plasticity [16]. Herein, we further investigated the role of LIF/ ZBTB46 signalling in stimulating expressions of glycolytic genes and altering the metabolic properties of PCa. We investigated the mechanisms of how inhibition of AR signalling promotes the process of glucose metabolism and therapeutic resistance to enable CRPC-NE development. Through cross-gene signatures and chromatin immunoprecipitation (ChIP) analyses, we identified LIF/ZBTB46 signalling as a key promoter of metabolic reprogramming and NE differentiation of PCa cells through interactions with PCK1. We identified the molecular basis of PCK1 specifically associated with therapeutic resistance following hormonal (anti-androgen or AR antagonist) therapy or leading to NE differentiation. We showed that ZBTB46 directly upregulates the expression of *PCK1* and NE marker gene through activation of LIF signalling. The upregulated PCK1 may reciprocally increase the expression of ZBTB46 that favours the expression of NE markers. We further surveyed putative PCK1 inhibitors from clinically approved drugs and examined their potential in vitro and in vivo effects on PCa. We demonstrated that genetic or pharmacological inhibition of PCK1 suppresses tumour growth in multiple models of AR-negative and NE-like cells, pointing to a potential approach for treating CRPC-NE.

METHODS

Cell culture and treatment

The LNCaP, VCaP, PC3, and LASCPC01 PCa cell lines used in this study were obtained from American Type Culture Collection (Manassas, VA, USA). Culture media for these cells were RPMI1640 (ThermoFisher, 11875085, Waltham, MT, USA) with 5% fetal bovine serum (FBS, Merck, TMS-013-BKR, Darmstadt, Germany) (LNCaP and LNCaP/MDVR), Dulbecco's modified Eagle medium (DMEM, ThermoFisher, 11965092) with 5% FBS (VCaP), RPMI1640 with 5% heat-inactivated FBS (PC3), and HITES medium (LASCPC01) [17]. In addition to these ingredients, 1 mM sodium pyruvate (ThermoFisher, 11360070), 1× non-essential amino acids (NEAAs, ThermoFisher, 11140050), 1× GlutaMAX (ThermoFisher, 35050061), and 1× penicillin/streptomycin (ThermoFisher, 15070063) were also added. The enzalutamide-resistant LNCaP/MDVR cell line is a clone derived from long-term treatment of LNCaP cells with 20 μM of enzalutamide (MDV3100, Selleckchem, S1250, Houston, TX, USA) for 12 months. Cells in the medium were cultured at 37 °C with 5% CO_2 and saturated humidity, and all cell lines were tested negative for mycoplasma contamination. Subculture of cells used 0.05% trypsin/EDTA (for all adherent cells) or centrifugation at 300 rpm for 5 min (for LASCPC01 cells). For low-glucose treatment, cells were incubated with glucose-free medium and 0.1 mM glucose (ThermoFisher, A2494001) overnight. For LIF (R&D Systems, 7734-LF, Minneapolis, MN, USA) and dihydrotestosterone (DHT) (Sigma-Aldrich, A8380, Darmstadt, Germany) administration, LIF or DHT was prepared in CSS-containing medium at respective concentrations of 100 and 2 ng/ml. Cells were incubated in a LIF-containing medium for 48 h. EC330 was purchased from Selleckchem (S0472, Pittsburgh, PA, USA). Nilotinib (HY-10159) and lapatinib (HY-50898) were all obtained from MedChemExpress (Monmouth Junction, NJ, USA). The cPEPCK inhibitor was purchased from Axon Medchem (Axon 1165, Reston, VA, USA).

Glycolytic flux analysis

LNCaP/EV- and LNCaP/ZBTB46-overexpressing cells (at 4×10^6) were seeded in 10-cm culture dishes, and incubated under culture conditions overnight to reach confluence. The next day, cells were treated with glucose-free RPMI1640 medium with all supplementation and an additional 1 g/l of glucose and 1 g/l of ^{13}C6-glucose (Sigma-Aldrich, 389374) for 24 and 48 h. Afterwards, cells were washed with PBS, detached with trypsin, counted, and resuspended in 1 ml PBS with equal cell numbers. Cell suspensions were used to analyse metabolic intermediates by liquid chromatography-tandem mass spectrometry (LC–MS/MS), and relative contents of metabolic intermediates in LNCaP/ZBTB46 cells are presented as the ratio to LNCaP/EV cells.

Assessment of the glycolytic rate

The glycolytic activity was monitored using a Seahorse XF24 analyzer (Agilent, Santa Clara, CA, USA) with a glycolytic rate test kit (Agilent, 103344-100) following the protocol in the manual. Target cells at 5×10^4 cells/well (at about 95% confluence) were inoculated into XF24 cell culture plates (Agilent, 100777-004) and cultured overnight until confluent. Then, cells were washed with FBS-free, phenol-red free, and glucose-free base medium (Agilent 103336-100) supplemented with HEPES (Agilent, 103337-100), 2 mM glutamine (Agilent, 103579-100), and 1 mM sodium pyruvate (Agilent, 103578-100). Then, the extracellular acidification rate (ECAR) value in each well was monitored with a Seahorse XF24 analyzer. The glycolytic rate in each well was automatically calculated by the analyzer.

Measurement of glucose consumption, lactate production, and intracellular pyruvate content

Glucose consumption (Abcam, ab65333, Cambridge, MA, USA), lactate production (Abcam, ab65331), and the intracellular pyruvate content (Abcam, ab65342) were measured with colorimetric assay kits following protocols in the respective manuals. Cells (4×10^6) were seeded in 10-cm culture dishes and appropriately treated for 24 h. Then, 1 ml of conditioned medium from each treatment was collected, precipitation was eliminated by centrifuging at 3000 rpm for 5 min, and the supernatant was used in a glucose consumption analysis. Any remaining attached cells were detached, washed with pre-warmed PBS, and lysed with assay buffer in the pyruvate assay kit as were the assay samples. To determine lactate production, 10^6 cells were seeded and cultured with 10 ml of culture medium for 24 h. Afterwards, a clear conditioned medium was collected as the assay sample.

Real-time quantitative reverse-transcription polymerase chain reaction (RT-qPCR) analysis

The protocol of RT-qPCR analysis was described in Supplementary Methods. Primers of the RT-qPCR programme used in this study are shown in Supplementary Table S1.

Immunoblotting

The protocol of immunoblotting analysis was described in Supplementary Methods. All antibodies are listed in Supplementary Table S2.

Chromatin immunoprecipitation (ChIP) assay

A ChIP assay was performed with an EZ-Magna ChIP™ IP kit A (Sigma-Aldrich, 17-10086) following the protocol in the manual, as described in Supplementary Methods. ChIP antibodies and qPCR primers are listed in Supplementary Table S3.

Promoter reporter assay

ZREs were located upstream of human *PCK1* on chromosome 20: 57555522 (ZRE1), 57559212 (ZRE2), 57559512 (ZRE3), and 57561020 (ZRE4) at GRCh38. These regulatory sequences with response element-GFP reporter vectors were constructed using the Clone-it Enzyme free Lentivector Kit (System Biosciences, Palo Alto, CA, USA). Response-element mutations were made using a Site-Directed Mutagenesis System kit (Invitrogen). The protocol of the promoter-reporter assay was described in Supplementary Methods. All primers used for constructs are listed in Supplementary Table S4.

Immunohistochemistry (IHC) staining

CRPC and SCPC TMAs were obtained from Duke University School of Medicine, and their use was approved by the Duke University School of Medicine Institutional Review Board (protocol ID: Pro00070193). Seventeen PCa tissue samples before and after ADT were collected from Taipei Medicine University-Wan-Fang Hospital (Taipei, Taiwan), the collection of which followed the Declaration of Helsinki and was approved by the Taipei Medical University Joint Institutional Review Board (protocol ID: N202103136). TMA and tumour slides were stained with PCK1 (1:100, Proteintech, 16754-1-AP, Rosemont, IL, USA), and a snapshot was taken with the Axioplan microscope system (Carl Zeiss, Oberkochen, Germany) at 200× magnification. The intensity of the tissue snapshot was denoted as 0 (negative), 1+ (weak positive), 2 (moderate positive), or 3+ (strong positive), and summarised into an H-index based on the following formula [18]: H index $= [1\times(\%\text{ cells of }1+)] + [2\times(\%\text{ cells of }2+)] + [3\times(\%\text{ cells of }3+)]$.

Immunofluorescence (IF) staining

Low- and high-grade PCa TMAs were obtained from Duke University School of Medicine. Slides were stained with PCK1 (1:400, Proteintech, 16754-1-AP) and ZBTB46 (1:400, Novus Biologicals, H00140685-B01P, Centennial, CO, USA). PCa TMA sections were washed with PBS containing 0.1% Tween-20, incubated with Alexa-488- and/or Alexa-568-conjugated immunoglobulin G (IgG) in 2% BSA for 30 min at room temperature, and finally washed and mounted using Fluoro-gel II anti-fade reagent with 4′,6-diamidino-2-phenylindole (DAPI) (Electron Microscopy Sciences, Hatfield, PA, USA). Fluorescent images were acquired using IXplore standard inverted microscopy (Olympus, Tokyo, Japan) and merged using ImageJ software.

Proliferation assay

PC3, PC3/shLuc, PC3/shZBTB46, and PC3/shPCK1 cells at 5×10^3 cells/well were inoculated into six 96-well culture plates and incubated overnight. The protocol of the proliferation assay was described in Supplementary Methods.

Sphere formation

In total, 500 cells/well was diluted with complete medium to 50 µl followed by mixed with an aliquot of Matrigel Matrix (Corning Life Sciences, Biocoat 354234, Corning, NY, USA). The protocol of the sphere formation assay was described in Supplementary Methods.

In vivo tumorigenic assay

Thirty 6-week-old NOD.CB17-*Prkdc*^{scid}/JNarl mice were obtained from the Genomics Research Center (Academia Sinica, Taipei, Taiwan) and randomised into six groups: three groups were inoculated with PC3 and the others were inoculated with LASCPC01 cells by a subcutaneous injection. Then, mice were intraperitoneally injected with dimethyl sulfoxide (DMSO), nilotinib (25 mg/kg), or lapatinib (30 mg/kg) once a week for 40 days in a double-blind situation. Mice body weights and tumour volumes were measured weekly. Mice were sacrificed via CO_2 anaesthetisation, and tumours were collected, weighed, sliced, and stained with PCK1, NE, and growth markers by IHC. The above-mentioned protocol was followed "Guideline for the Care and Use of Laboratory Animals" published by the Council of Agriculture and approved by Taipei Medical University Institutional Animal Care and Use Committee (approval ID LAC-2021-0111).

Statistical analysis

All experiments were averaged from at least three independent experiments. All plots were made with GraphPad Prism V8.01 (La Jolla, CA, USA) followed by an analysis of statistical significance using an analysis of variance (ANOVA) coupled with Dunnett's test, when compared to the desired control. For comparison of IHC staining of ADT samples, paired Student's *t*-test with two-tailed tests was performed.

RESULTS

ZBTB46 and LIF upregulation activates glucose metabolism in PCa

We recently identified ZBTB46 as a tumour promoter for PCa metastasis [19]. Despite abnormal increases in glycolysis being related to the malignant progression of PCa [6], it is unclear whether ZBTB46 is a regulator of glycolysis. To examine how increased ZBTB46 expression affects glucose catabolism, we labelled AR-positive LNCaP cells with ^{13}C6-glucose and evaluated total levels and levels of ^{13}C-labelled metabolites by liquid chromatography-tandem mass spectrometry (LC–MS/MS). Results showed that labelled profiles of PEP, pyruvate, and lactate were much higher in ZBTB46-overexpressing cells (Fig. 1a). We further analysed the extracellular acidification rate (ECAR) in cells with ZBTB46 overexpression on a Seahorse XF24 extracellular flux analyzer to detect glycolytic flux in cells, and found that ZBTB46-overexpressing cells demonstrated an increase in the ECAR compared to control cells (Fig. 1b). These results support ZBTB46 upregulation increasing glucose metabolic processes in PCa cells. ZBTB46 is known to be activated by LIF signalling in PCa tumours after ADT [16]. We further tested whether PCa cells activate LIF/ZBTB46 signalling in low-glucose conditions to modulate metabolic processes. LNCaP cells were treated with decreasing concentrations of glucose, and relative levels of LIF and ZBTB46 were analysed. Interestingly, we found that cells under low-glucose treatment had higher LIF and ZBTB46 expressions (Fig. 1c). In addition, cells treated with the LIF protein had increased ZBTB46 expression, and more ZBTB46 was found in ZBTB46-expressing cells with LIF overexpression (Fig. 1d). In contrast, ZBTB46 upregulation was eliminated in cells with ZBTB46-knockdown (KD) regardless of LIF treatment (Fig. 1e), supporting the existence of crosstalk between ZBTB46 and LIF [16]. We further analysed relative levels of metabolic products to clarify if LIF functions by mediating ZBTB46-driven glucose metabolism in PCa cells via measuring amounts of lactate and pyruvate using a colorimetric assay. Significantly, cells overexpressing ZBTB46 showed increased glucose consumption, lactate secretion, and pyruvate levels compared to control cells, and LIF treatment produced additional stimulation (Fig. 1f). Moreover, results validated that ZBTB46-KD cells showed decreased glucose consumption and lactate and pyruvate levels and an abolition of the effect of LIF treatment on cells (Fig. 1g), suggesting the role of LIF/ZBTB46 signalling in regulating glucose metabolism. To identify the functional role of LIF/ZBTB46 signalling and its effects on cell proliferation, the cell growth rate and level of metabolic stress were evaluated. Results showed that although LIF treatment synergistically increased ZBTB46-driven cell viability (Fig. 1h), ZBTB46-KD cells exhibited a decreased effect of LIF-driven cell viability (Fig. 1i). Furthermore, ZBTB46-overexpressing cells demonstrated increased ECAR compared to control cells, and LIF-treated cells exhibited an additional increase in the ECAR value (Fig. 1j). In contrast, ZBTB46-KD cells showed a decrease in ECAR even in cells with LIF treatment (Fig. 1k). These data suggest that upregulation of LIF/ZBTB46 signalling is associated with activation of the glucose metabolic pathway to support PCa cell proliferation.

LIF/ZBTB46 signalling promotes glucose metabolism through upregulating PCK1

To determine the target of LIF/ZBTB46 signalling in altering the metabolic properties of PCa, we analysed relationships of LIF

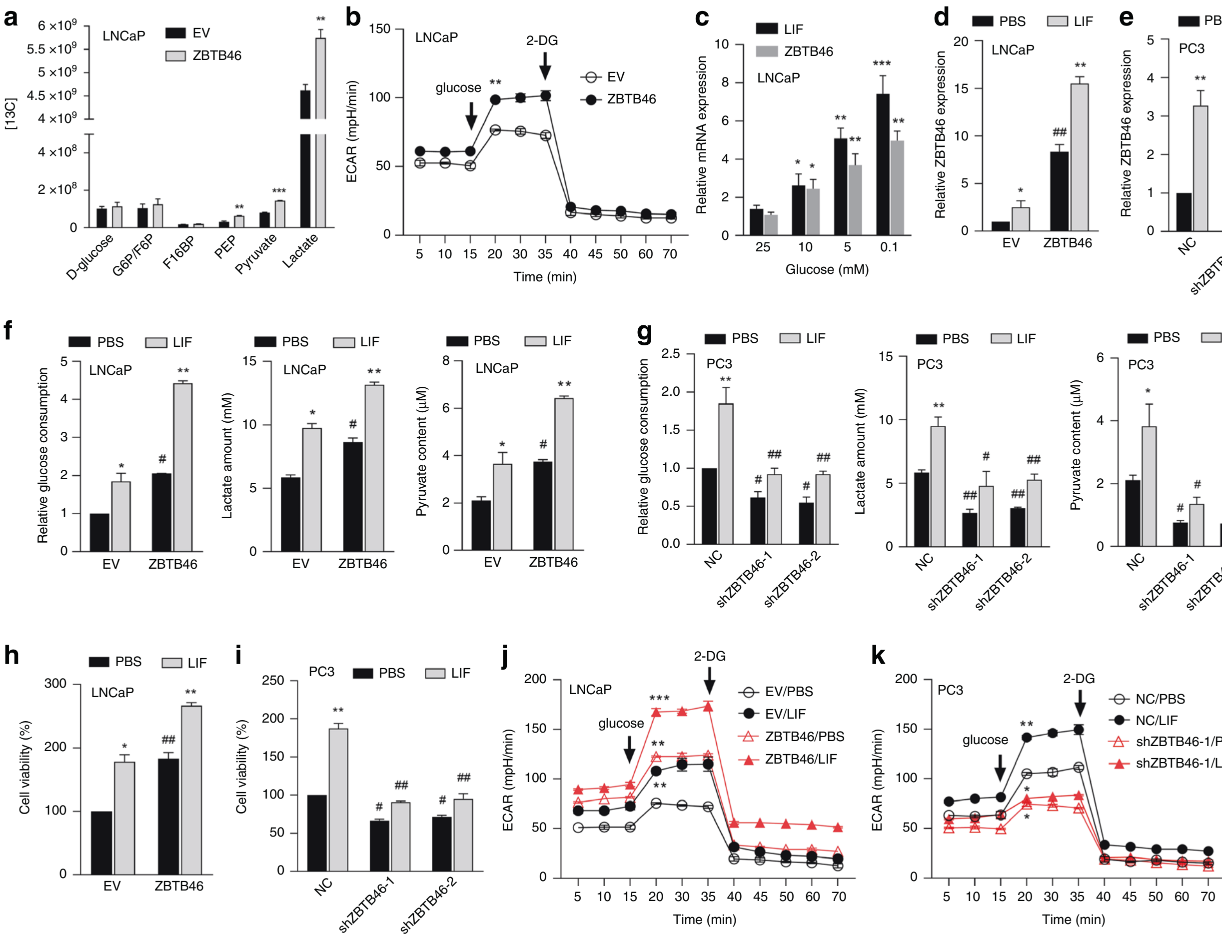

Fig. 1 LIF signalling enhances ZBTB46-driven glucose metabolism of PCa. **a** Relative abundance of ^{13}C6-labelled D-glucose, G6P/F6P, F16BP, PEP, pyruvate, and lactate derived from glucose from LNCaP cells with empty vector (EV) or ZBTB46 cDNA vector overexpression. * vs. EV. $^{**}p < 0.01$ and $^{***}p < 0.001$ by a *t*-test. **b** Bioenergetics trace from the Seahorse analysis showing the glycolysis stress test in the EV- or ZBTB46 cDNA vector-overexpressing LNCaP cells exposed to D-glucose (12 mM) and 2-deoxyglucose (2-DG) (50 mM). $n = 3$ biological replicates per group. * vs. EV. $^{**}p < 0.01$ by a *t*-test. **c** Relative ZBTB46 and LIF mRNA levels in LNCaP cells treated with various concentrations of glucose (0.1, 5, 10, and 25 mM). * vs. 25 mM glucose. $^{*}p < 0.05$, $^{**}p < 0.01$, and $^{***}p < 0.001$ by a *t*-test. **d**, **e** Relative ZBTB46 mRNA levels in LNCaP cells expressing the EV or ZBTB46 cDNA vector (**d**) or PC3 cells expressing the non-target control (NC) or ZBTB46 shRNA vector (**e**), and exposed to the LIF protein (100 ng/ml) for 24 h. Values are expressed as the multiple of change from the PBS-treated control group for EV- or NC shRNA vector-transfected cells. $n = 3$ biological replicates per group. * vs. PBS; # vs. the EV or NC. $^{*}p < 0.05$, $^{**}p < 0.01$, and $^{***}p < 0.001$ by a *t*-test. **f**, **g** Quantification of glucose uptake, lactate amount, and pyruvate content by a colorimetric assay of LNCaP cells expressing the EV or ZBTB46 cDNA vector (**f**), and PC3 cells expressing the NC or ZBTB46 shRNA vector (**g**), and incubated with the LIF protein (100 ng/ml) for 24 h, respectively. $n = 3$ biological replicates per group. $^{*}p < 0.05$, $^{**}p < 0.01$, and $^{***}p < 0.001$ by a *t*-test. **h**, **i** Viability curves for LNCaP cells expressing the EV or ZBTB46 cDNA vector (**h**) and PC3 cells expressing the NC or ZBTB46 shRNA vector (**i**), and incubated with the LIF protein (100 ng/ml) for 24 h, respectively. $n = 10$ biological replicates per group. * vs. PBS; # vs. the EV or NC. $^{*}p < 0.05$ and $^{**}p < 0.01$ by a *t*-test. **j**, **k** Bioenergetics trace from the Seahorse analysis showing the glycolysis stress test in LNCaP cells expressing the EV or ZBTB46 cDNA vector (**j**), and PC3 cells expressing the NC or ZBTB46 shRNA vector (**k**) exposed to the LIF protein (100 ng/ml) and treated with D-glucose (12 mM) and 2-DG (50 mM), respectively. $n = 3$ biological replicates per group. * vs. EV/PBS or NC/PBS. $^{*}p < 0.05$, $^{**}p < 0.01$, and $^{***}p < 0.001$ by a *t*-test.

and ZBTB46 expressions with glucose metabolic gene signatures validated by a *z*-score analysis and gene set enrichment analysis (GSEA) of The Cancer Genome Atlas (TCGA) PCa dataset [20]. We observed significant correlations of upregulated ZBTB46 and LIF expressions with increased glycolysis, the TCA cycle, and glucose metabolism response signatures in patients (Supplementary Fig. S1A, B). We focused on the effect of LIF/ZBTB46 signalling on glucose metabolism, and found that tissues expressing high levels of LIF and ZBTB46 were positively correlated with responsive gene signatures of glucose metabolism (Supplementary Fig. S1C). To filter marker selection and explore visual data, we applied a normalised enrichment score (NES) from both GSEA results to a differential expression analysis via hierarchical clustering. Based on the significance of the false discovery rate (FDR) and *p* values from GSEA results, we found that *SDS, ATF3, TNF, PCK1*, and *HK3* were present in the same cluster that was upregulated in both assays, where they were included in the top genes activated in response to both LIF and ZBTB46 upregulation (Supplementary Fig. S1D). We thus analysed expressions of these genes upon LIF treatment in PCa cells. LNCaP cells were treated with increasing concentrations of the LIF protein, and we found that those genes were stimulated after LIF treatment (Supplementary Fig. S1E). Moreover, PCK1 was the most significantly increased gene compared to other genes in cells overexpressing ZBTB46 and LIF (Supplementary Fig. S1F). These data indicate that PCK1 upregulation is related to activation of the glucose metabolism pathway regulated by LIF/ZBTB46 signalling.

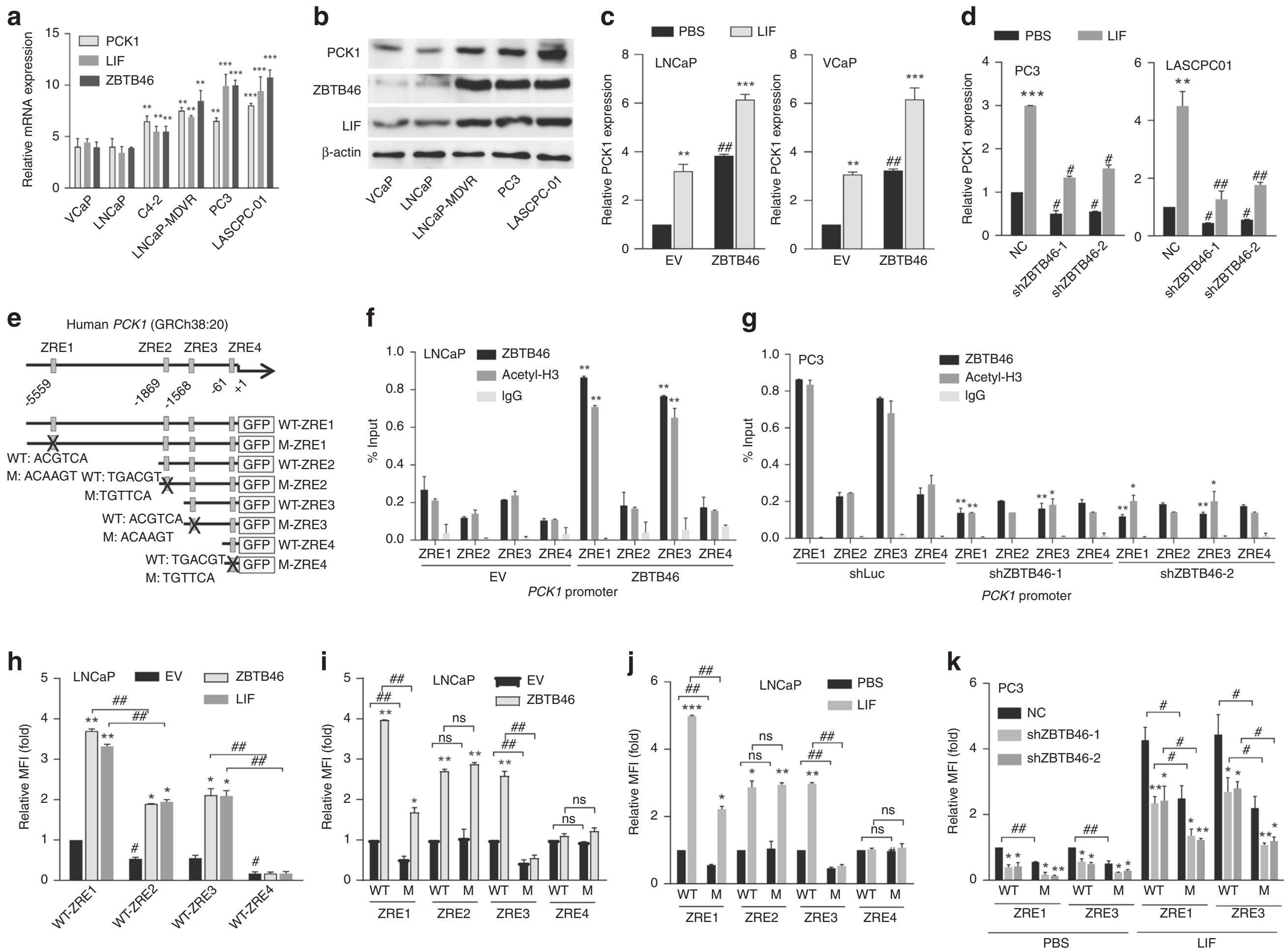

Fig. 2 PCK1 is upregulated by LIF/ZBTB46 in PCa cells. **a** Relative PCK1, LIF, and ZBTB46 mRNA expressions in various PCa cell lines. Values are expressed as the multiple of change compared to VCaP cells. $n = 3$ biological replicates per group. **$p < 0.01$ and ***$p < 0.001$ by a *t*-test. **b** Representative immunoblots of PCK1, ZBTB46, and LIF protein levels in various PCa cells. **c**, **d** Relative PCK1 mRNA levels in LNCaP and VCaP cells expressing an empty vector (EV) or ZBTB46 cDNA vector (**c**) or PC3 and LASCPC01 cells expressing the non-target control (NC) or ZBTB46 shRNA vector (**d**), and exposed to the LIF protein (100 ng/ml). Values are expressed as the multiple of change compared to the PBS-treated control group for the EV- or NC shRNA vector-transfected cells. $n = 3$ biological replicates per group. **$p < 0.01$ and ***$p < 0.001$ by a *t*-test. **e** Top: Schematic of the predicted ZBTB46 response elements (ZREs) in the regulatory sequence of human *PCK1*. Bottom: Schematic of *PCK1* regulatory sequence reporter constructs showing the wild-type (WT) and mutant (M) sequences of ZRE1 to ZRE4. **f**, **g** ChIP assays of LNCaP cells expressing the EV or ZBTB46 cDNA vector (**f**) and PC3 cells expressing the NC or ZBTB46 shRNA vector (**g**). An antibody against acetyl-H3 served as the positive control. Enrichment is given as a percentage of the total input and then normalised to IgG. $n = 3$ biological replicates per group. * vs. the EV or NC. *$p < 0.05$, **$p < 0.01$, and ***$p < 0.001$ by a *t*-test. **h** Relative median fluorescent intensity (MFI) of *PCK1* reporters (WT-ZRE1~WT-ZRE4) in LNCaP cells after transfection with the EV, ZBTB46, or LIF expression vector. * vs. the EV; # vs. WT-ZRE1 or WT-ZEB3. **i**, **j** Relative MFIs of *PCK1* reporters (WT-ZRE1~WT-ZRE4 and M-ZRE1~M-ZRE4) in LNCaP cells expressing the EV or ZBTB46 expression vector (**i**) or exposed to PBS or 100 ng/ml LIF protein for 24 h (**j**). * vs. the EV (**i**) or PBS (**j**); # vs. WT-ZREs. *$p < 0.05$, **$p < 0.01$, and ***$p < 0.001$ by a *t*-test. **k** Relative MFIs of *PCK1* reporters (WT-ZRE1, M-ZRE1, WT-ZRE3, and M-ZRE3) in PC3 cells expressing the NC or ZBTB46 shRNA vector, and exposed to PBS or the 100 ng/ml LIF protein for 24 h. * vs. the NC; # vs. WT-ZREs. *$p < 0.05$, **$p < 0.01$, and ***$p < 0.001$ by a *t*-test. Data from relative MFIs of *PCK1* reporters are the mean ± SEM of three independent experiments.

PCK1 is upregulated by LIF/ZBTB46 signalling in PCa cells

Next, we analysed PCK1 expression in various PCa cell lines, and observed that PCK1 messenger (m)RNA and protein levels were associated with ZBTB46 and LIF, and increased in the ADT-resistant LNCaP-MDVR cell line (enzalutamide-resistant clones derived from LNCaP cells), the AR-negative PC3 cell line, and the NE-like LASCPC01 cell line compared to the AR-positive VCaP, LNCaP, and C4-2 cell lines (Fig. 2a, b). We next examined the relationship between activation of LIF/ZBTB46 signalling in regulating PCK1 expression. We observed a synergistic increase of PCK1 mRNA in ZBTB46-overexpressing LNCaP and VCaP cells incubated with the LIF protein (Fig. 2c); however, those effects were abolished in PC3 and LASCPC01 cells expressing ZBTB46-KD, regardless of LIF treatment (Fig. 2d). These data suggest that PCK1 upregulation is associated with LIF signalling for which ZBTB46 is required. We searched for sequences resembling the putative ZBTB46 response element (ZRE) [21] in the *PCK1* regulatory sequence region. Notably, we found there were four candidate ZREs for nuclear ZBTB46 at nucleotides −5559, −1869, −1568, and −61 relative to the *PCK1* transcriptional start site (Fig. 2e). We hypothesised that activated LIF/ZBTB46 signalling induces PCK1 expression, and its involvement in glucose metabolism may be mediated by a direct interaction between nuclear ZBTB46 and the *PCK1* regulatory sequence. ChIP assays were performed to validate enrichment of ChIP products using a ZBTB46 antibody and a positive control acetyl-H3 antibody at the putative ZREs in the *PCK1* regulatory sequence in AR-positive LNCaP cells stably transfected with ZBTB46 complementary (c)DNA. Results showed that the ZRE1 and ZRE3 sites had enhanced binding abilities for ZBTB46 compared to the others (Fig. 2f). We also observed a decrease in ZBTB46 binding activity at the ZRE1 and ZRE3 sites in response to ZBTB46-KD in AR-negative PC3 cells (Fig. 2g). We further performed reporter assays with a DNA construct containing serial deletions of the *PCK1* promoter cloned into the promoter of a green fluorescence protein (GFP) reporter gene. ZBTB46- or LIF-cDNA-overexpressing cells showed significant increases in *PCK1* reporter activity at the ZRE1, ZRE2, and ZRE3 sites, while none was seen at the ZRE4 site (Fig. 2h). We also found that deletion of fragments containing the ZRE1 and ZRE3 sites significantly reduced the activity of the *PCK1* reporter gene (Fig. 2h), supporting these two sites having enriched binding abilities for ZBTB46. Moreover, we used a *PCK1*-GFP reporter construct in which the putative ZREs were mutated (Fig. 2e). Although ZBTB46 or LIF overexpression induced reporter gene activity at wild-type (WT) ZRE1, ZRE2, and ZRE3 in the presence of a ZBTB46-expressing vector or the LIF protein, mutations at the ZEB1 and ZEB3 sites demonstrated significant reductions in reporter gene activities (Fig. 2i, j). In addition, there was no significant change in the activity of the reporter with mutations of ZEB2 and ZEB4 compared to the WT reporters regardless of ZBTB46 or LIF overexpression (Fig. 2i, j). Moreover, decreased reporter activity was detected when the WT ZRE1 and ZRE3 reporter constructs were co-transfected with the ZBTB46 small hairpin (sh)RNA vector in PC3 cells (Fig. 2k). We also found increased reporter activity in cells harbouring the WT reporters with LIF protein treatment; however, the mutants and ZBTB46 shRNA vector decreased the effects of the LIF protein (Fig. 2k). These results are consistent with our hypothesis that activation of LIF/ZBTB46 signalling upregulates PCK1 through a direct interaction between ZBTB46 and the *PCK1* gene.

ADT induces PCK1 expression, which is associated with NE differentiation of PCa

Our previous study showed that activation of LIF/ZBTB46 signalling is involved in NE differentiation of PCa after ADT [16]. We further studied the clinical association between LIF/ZBTB46 and PCK1 in the progression to CRPC-NE. LNCaP cells were treated with androgen deprivation (charcoal-stripped serum (CSS)-containing medium) to mimic ADT. Results showed that induction of PCK1 expression was associated with increased levels of NE markers (*CHGA, ENO2*, and *SYP*), but reduced expressions of androgen-responsive genes (*NKX3-1* and *KLK3*) (Fig. 3a). In contrast, decreased levels of PCK1 and NE markers and increased levels of androgen-responsive genes were observed in cells treated with the AR ligand, dihydrotestosterone (DHT) (Fig. 3a). Moreover, NE marker expression decreased in cells expressing PCK1-KD, regardless of CSS-containing medium treatment (Fig. 3b). Consistently, mRNA expression profile data from LNCaP cells cultured during 11 months of androgen deprivation revealed a significant increase in PCK1 expression after androgen deprivation (GDS3358, Fig. 3c). We collected PCa tissues from the same PCa patients before and after ADT to assess whether PCK1 upregulation is mediated by ADT. Significantly, PCa tissues from the same PCa patients after ADT showed increased PCK1 levels compared to the same patients before ADT based on IHC analyses (Fig. 3d). Expression profiles from the same patients treated before and after ADT were validated and showed similar results (GSE48403, Fig. 3e). Importantly, LIF protein treatment of AR-positive LNCaP and VCaP cells showed increased levels of PCK1 associated with induction of ZBTB46 and NE markers, and reduced NKX3-1 expression (Fig. 3f), whereas PCK1-KD abolished effects of the LIF (Fig. 3g). These data suggest that PCK1 upregulation is related to LIF/ZBTB46-mediated NE differentiation of PCa cells after ADT. In addition, PCK1-KD in PC3 and LASCPC01 cells showed reductions in ZBTB46 and NE markers (Fig. 3h, i), suggesting that PCK1 reciprocally modulates ZBTB46 expression. To further evaluate the effect of PCK1 mediation of ZBTB46 and NE differentiation on PCa, an inducible Tet-PCK1 vector was expressed in LNCaP cells. Results showed that cells with doxycycline (Dox) treatment exhibited PCK1 upregulation, which was associated with increased mRNA and protein levels of ZBTB46 and NE markers, and decreased androgen-responsive gene expressions (Fig. 3j, k), supporting the positive feedback of PCK1 on ZBTB46 expression. Importantly, ZBTB46-KD in LNCaP/Tet-PCK1 cells in the presence of Dox showed decreases in NE markers and increases in androgen-responsive gene expressions compared to cells with non-target control (NC) shRNA expression (Fig. 3l, m). Moreover, parental LNCaP cells with ZBTB46-KD following LIF protein treatment also produced decreases in PCK1 and NE markers, and increases in androgen-responsive gene expressions (Fig. 3n, o), supporting PCK1-induced NE differentiation being required for LIF/ZBTB46 signalling activation. Based on these results, ADT-induced PCK1 associated with NE differentiation in PCa is ZBTB46 dependent.

LIF-induced and PCK1-stimulated ZBTB46 upregulates *SYP, CHGA*, and *ENO2*

We sought to determine whether the signalling profile that characterises PCK1 expression which promotes NE differentiation of PCa is required for LIF/ZBTB46 signalling. Interestingly, based on the transcription factor search programme, there were individual putative ZREs [21] in the regulatory sequences of *CHGA, ENO2*, and *SYP* (Fig. 4a). We hypothesised that ZBTB46 may act as a transcriptional activator of NE markers through binding to the *CHGA, ENO2*, and *SYP* regulatory sequences. ChIP assays validated that the binding abilities of ZBTB46 to the putative ZREs of *CHGA, ENO2*, and *SYP* regulatory sequences increased in LNCaP-Tet-PCK1 cells after Dox treatment; however, binding abilities decreased in cells with ZBTB46-KD (Fig. 4b), suggesting that the binding ability of ZBTB46 is associated with PCK1 upregulation. Consistently, the endogenous binding of ZBTB46 to the *SYP*, *CHGA*, and *ENO2* regulatory sequences increased in cells after LIF treatment, and decreased in cells with ZBTB46-KD, regardless of LIF treatment (Fig. 4c), suggesting that LIF signalling can upregulate ZBTB46 binding to the *SYP*, *CHGA*, and *ENO2* regulatory sequences. Moreover, the binding activities of ZBTB46 with the regulatory sequences of *CHGA, ENO2*, and *SYP* decreased in cells with LIF inhibitor (EC330) [16] treatment (Fig. 4d). These observations confirmed that physical interactions of ZBTB46 with regulatory sequences of NE markers are stimulated by LIF signalling and PCK1 activation. We further performed a promoter-reporter assay using a GFP reporter-containing individual ZREs located at the regulatory sequences of *CHGA, ENO2*, and *SYP*. Interestingly, LNCaP-Tet-PCK1 cells with Dox treatment showed increases in *CHGA, ENO2*, and *SYP*-reporter activities compared to control cells, but ZBTB46-KD abolished those effects (Fig. 4e). Similarly, PC3 cells under LIF activation also revealed increases in *CHGA, ENO2*, and *SYP*-reporter activities; however, these reporter activities decreased in cells with ZBTB46-KD (Fig. 4f). Moreover, the reporter assays showed that the LIF inhibitor or the *CHGA-, ENO2-*, and *SYP*-reporter mutants could eliminate LIF protein-driven reporter activity in cells (Fig. 4g). Furthermore, reporter activity increased in cells with exogenous ZBTB46 overexpression, and synergistically upregulated reporter activity was found in ZBTB46-expressing cells after LIF treatment (Fig. 4h), whereas mutants abolished this effect. In summary, these data indicate that stimulation of LIF and PCK1 can induce NE differentiation of cells that require activation of ZBTB46, which directly mediates the transcriptional activity of the *SYP*, *CHGA*, and *ENO2* genes.

Upregulation of PCK1 is associated with PCa aggressiveness

In studying the clinical relevance of PCK1, we used a tissue microarray (TMA) obtained from the Department of Pathology at Duke University School of Medicine (Durham, NC, USA), which was

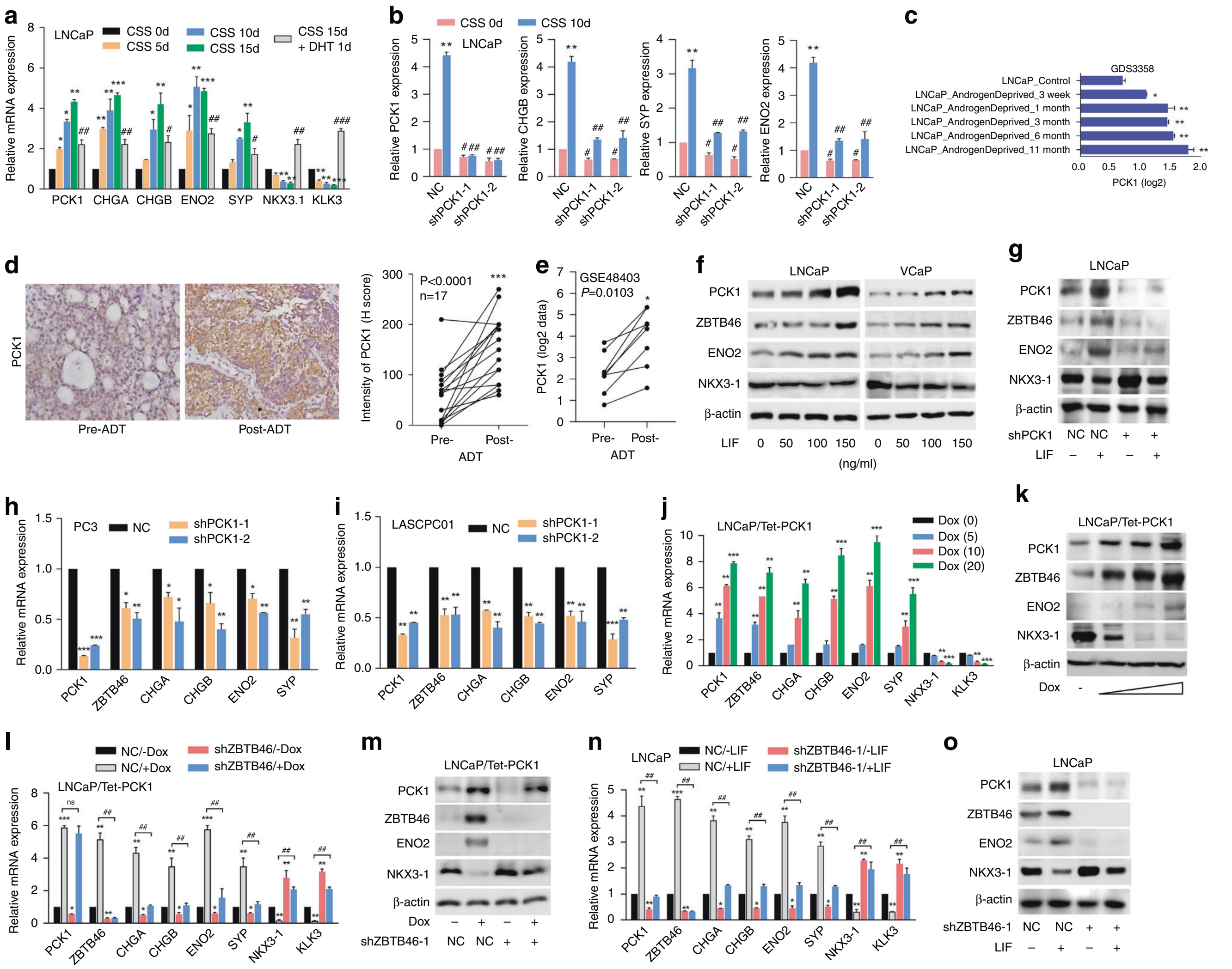

Fig. 3 ADT increased PCK1 expression, which promotes NE differentiation of PCa cells through LIF/ZBTB46 signalling upregulation. **a** Relative mRNA expression of PCK1, NE markers (*CHGA, CHGB, ENO2*, and *SYP*), and AR-related genes (*NKX3-1* and *KLK3*) in LNCaP cells treated with CSS-containing medium for 0, 5, 10, and 15 days, and treated with DHT (2 ng/ml) for 1 day. Values are expressed as the multiple of change compared to cells treated with CSS on day 0. $n = 3$ biological replicates per group. $^{**}p < 0.01$ and $^{***}p < 0.001$ by a *t*-test. **b** Relative PCK1 and NE marker mRNA expressions in LNCaP cells expressing the non-target control (NC) or PCK1 shRNA vector, and treated with CSS-containing medium for 0 and 10 days. * vs. CSS 0 d; # vs. the NC. $^{*}p < 0.05$, $^{**}p < 0.01$, and $^{***}p < 0.001$ by a *t*-test. **c** Expression of PCK1 in LNCaP cells from the GDS3358 database during 11 months of androgen deprivation. * vs. LNCaP_Control. $^{*}p < 0.05$ and $^{**}p < 0.01$ by a *t*-test. **d** IHC staining showing images and intensities of cytoplasmic PCK1 in PCa tissue sections from the same patients before and after ADT. The 17 samples were collected from Taipei Medical University-Wan Fang Hospital. Scale bars, 100 μm. Statistical analysis was performed by a two-tailed Student's *t*-test. $^{***}p < 0.001$. **e** Expressions of PCK1 in paired PCa samples pre- and post-ADT from the GSE48403 dataset. Statistical analysis was performed by a two-tailed Student's *t*-test. $^{*}p < 0.05$. **f** Representative immunoblots of PCK1, ZBTB46, ENO2, and NKX3-1 protein levels in LNCaP and VCaP cells exposed to various concentration of the LIF protein for 48 h. **g** Representative immunoblots of PCK1, ZBTB46, ENO2, and NKX3-1 protein levels in LNCaP cells expressing the NC or PCK1 shRNA vector and treated with the LIF protein (100 ng/ml) for 48 h. **h**, **i** Relative PCK1, ZBTB46, and NE marker mRNA expressions in PC3 (**h**) or LASCPC01 (**i**) cells expressing the NC or PCK1 shRNA vector. **j** Relative PCK1, ZBTB46, CHGA, CHGB, ENO2, SYP, NKX3-1, and KLK3 mRNA expressions in LNCaP/Tet-PCK1 cells exposed to various concentrations of doxycycline (Dox, 0, 5, 10, and 20 ng/ml). * vs. Dox (0). **k** Representative immunoblots of PCK1, ZBTB46, ENO2, and NKX3-1 protein levels in LNCaP/Tet-PCK1 cells exposed to various concentration of Dox. l, m Relative PCK1, ZBTB46, NE marker, and AR-related gene mRNA (**l**) and protein (**m**) expressions in LNCaP/Tet-PCK1 cells expressing the NC or ZBTB46 shRNA vector, and exposed to Dox (20 ng/ml) for 48 h. * vs. NC/−Dox; # vs. NC/+Dox. n, o Relative mRNA (**n**) and protein (**o**) expressions of PCK1, ZBTB46, NE markers, and AR-related genes in LNCaP cells expressing the NC or ZBTB46 shRNA vector, and exposed to LIF (100 ng/ml) for 48 h. * vs. NC/-LIF; # vs. NC/+LIF. $^{**}p < 0.01$ and $^{***}p < 0.001$ by a *t*-test. Data from relative mRNA expression are the mean ± SEM of three independent experiments.

composed of normal tissues ($n = 16$), adenocarcinomas with a Gleason score of ≤7 ($n = 81$), adenocarcinomas with a Gleason score of ≥8 ($n = 19$), and the more-aggressive SCPC ($n = 8$), to determine PCK1 expression during PCa progression. Interestingly, increased PCK1 expression was observed in high-grade tumours and most SCPC cases compared to low-grade and normal tissues as validated by IHC staining (Fig. 5a, b). Correlations with mean expression levels were confirmed in a PCa dataset (GSE21036) [22], showing that PCK1 was upregulated in samples with high metastatic potential (Fig. 5c) and high Gleason scores (Fig. 5d). Moreover, samples with high PCK1 expression exhibited low survival rates (Fig. 5e). Importantly, levels of PCK1 were higher in patients with CRPC-NE compared to patients with an adenocarcinoma in the CRPC-NE-responsive dataset [23] (Fig. 5f). According

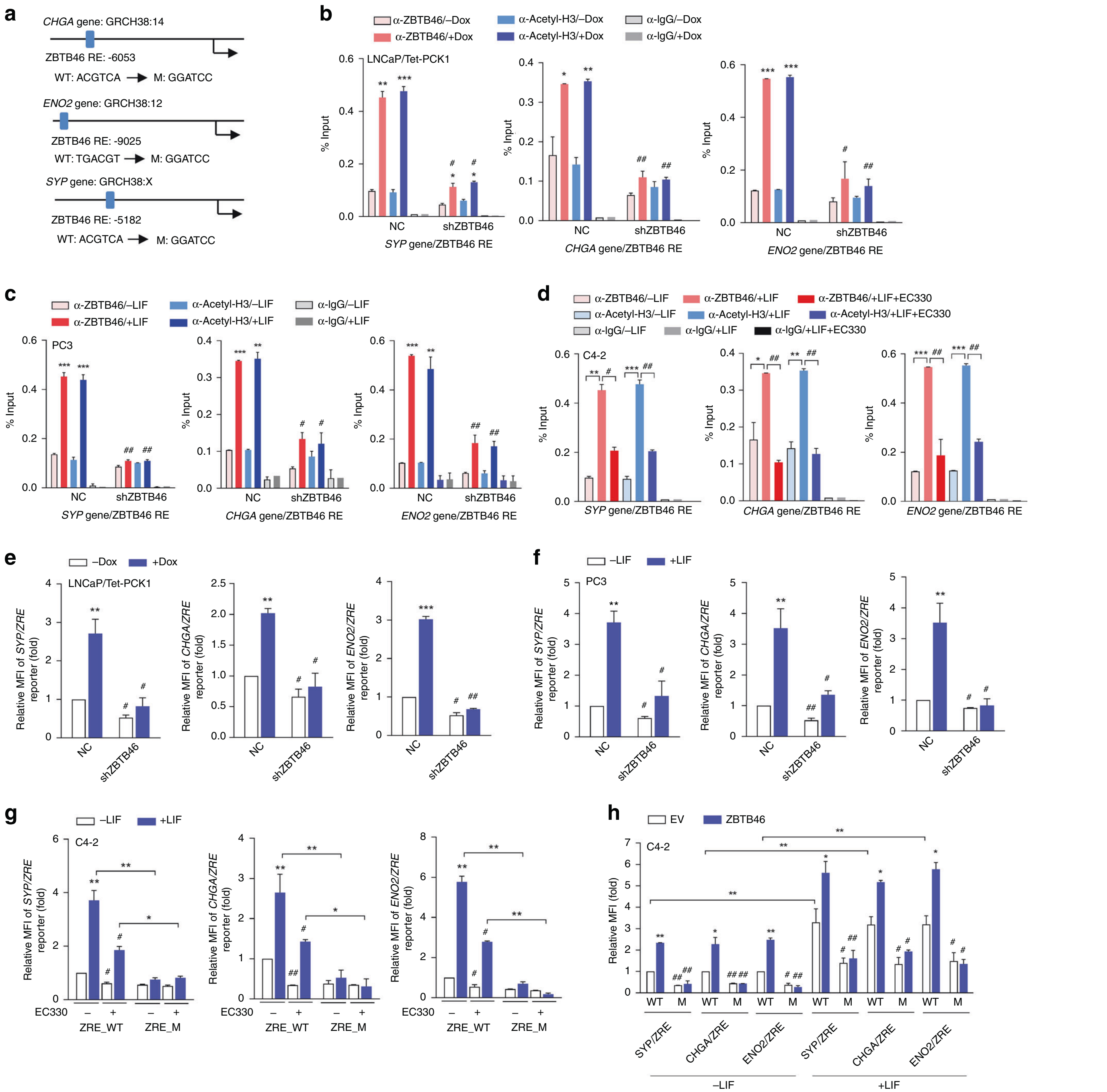

Fig. 4 PCK1 and LIF upregulate ZBTB46, and ZBTB46 directly binds *CHGA, ENO2*, and *SYP* regulatory sequences. **a** Schematic of the predicted ZBTB46-regulatory elements (ZREs) in the regulatory sequence of human *CHGA, ENO2*, and *SYP*, showing the sequences of the wild-type (WT) and mutant (M) ZREs on the *CHGA, ENO2*, and *SYP* genes. **b**, **c** ChIP assays of the non-target control (NC) or ZBTB46 shRNA stably transfected LNCaP/Tet-PCK1 (**b**) or PC3 (**c**) cells following 20 ng/ml of doxycycline (Dox) (**b**) or 100 ng/ml LIF protein (**c**) treatment for 24 h using specific antibodies against ZBTB46 and acetyl-H3, or control IgG for IP. Precipitated DNA was quantified via a quantitative (q)PCR of ZREs among regulatory sequences of *CHGA, ENO2*, and *SYP*. Enrichment is given as a percentage of the total input. * vs. -Dox (**b**) or -LIF (**c**); # vs. the NC. **d** ChIP assays of C4-2 cells with 100 ng/ml LIF or combined with 10 μM EC330 treatment for 24 h using specific antibodies against ZBTB46 and acetyl-H3, or control IgG. * vs. -LIF; # vs. +LIF. **e**, **f** Relative medium fluorescent intensities (MFIs) of *SYP, CHGA*, and *ENO2* reporters in LNCaP/Tet-PCK1 (**e**) or PC3 (**f**) cells following treatment with 20 ng/ml of Dox (**e**), or 100 ng/ml LIF protein (**f**). * vs. -Dox (**e**) or -LIF (**f**); # vs. the NC. **g** Relative MFIs of WT-ZRE or M-ZRE of *SYP, CHGA*, and *ENO2* reporters in C4-2 cells with 100 ng/ml LIF or combined with 10 μM EC330 treatment for 24 h. * vs. -LIF; # vs. -EC330. **h** Relative MFIs of WT-ZRE or M-ZRE of *SYP, CHGA*, and *ENO2* reporters in C4-2 cells with 100 ng/ml LIF treatment for 24 h following stable transfection with the empty vector (EV) or ZBTB46 cDNA vector. * vs. the EV or -LIF; # vs. the WT-ZREs. Data from relative ChIP and MFIs of *PCK1* reporters are the mean ± SEM of three independent experiments. *$p < 0.05$, **$p < 0.01$, and ***$p < 0.001$ by a *t*-test.

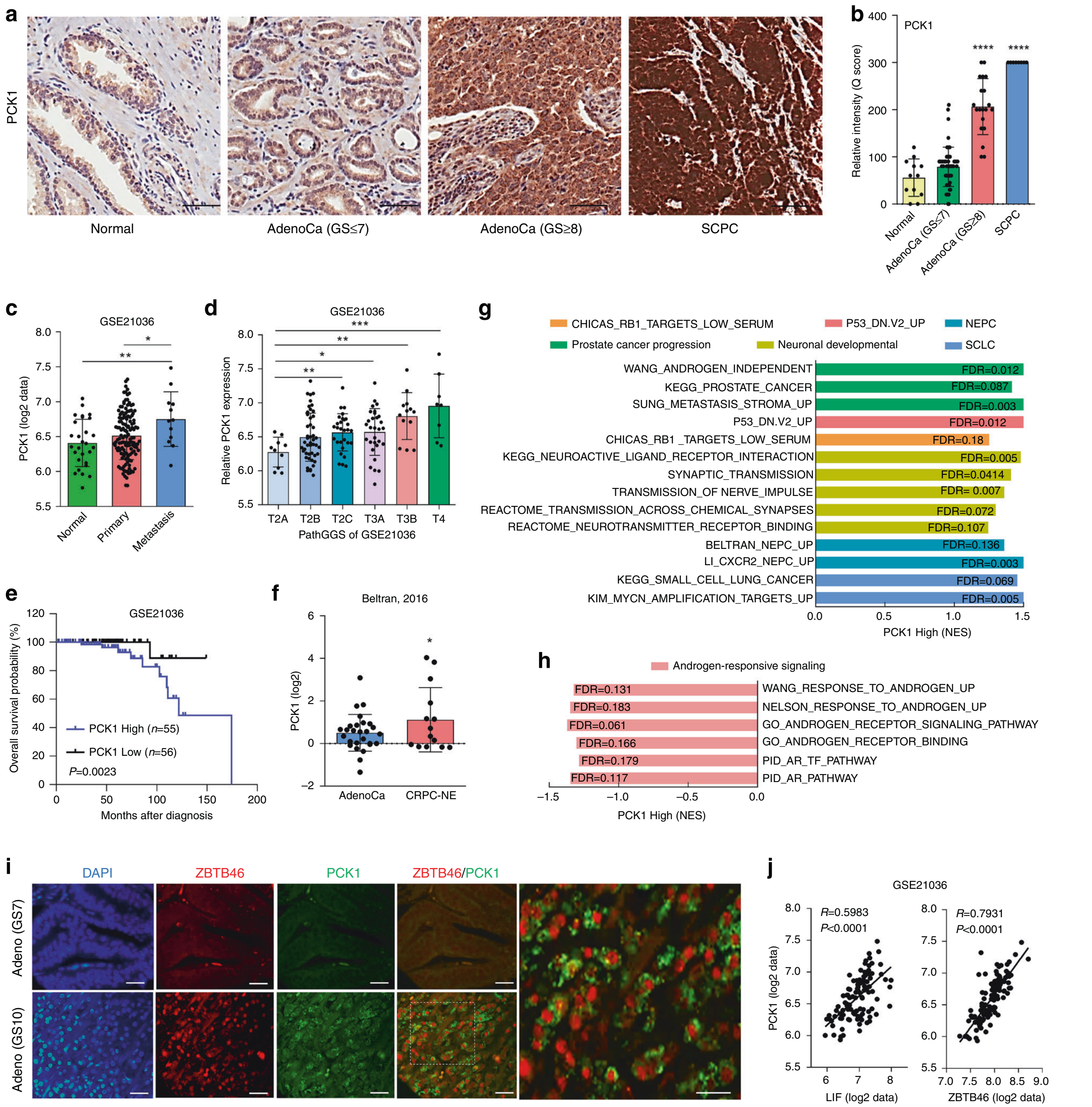

Fig. 5 PCK1 upregulation is associated with NE-differentiated PCa. a, b IHC staining (**a**) and relative intensities (**b**) of PCK1 expression in a PCa TMA, including normal tissues ($n = 16$), adenocarcinomas (AdenoCas) with a Gleason score of ≤7 ($n = 81$), AdenoCas with a Gleason score of ≥8 ($n = 19$), and SCPC samples ($n = 8$) from Duke University School of Medicine. * vs. normal tissues. ****$p < 0.0001$; by a one-way ANOVA. **c** Mean levels of PCK1 mRNA in normal ($n = 28$), primary ($n = 98$), and metastatic ($n = 13$) human prostate samples from the GSE21036 dataset. * vs. normal tissues. *$p < 0.05$ and **$p < 0.01$ by a one-way ANOVA. **d** Mean levels of PCK1 mRNA of various pathologic Gleason scores from the GSE21036 dataset. *$p < 0.05$, **$p < 0.01$, and ***$p < 0.001$ by a one-way ANOVA. **e** Kaplan–Meier analyses of PCK1 alterations in the GSE21036 dataset. A log-rank test was used for the survival curve analysis. **f** Comparison of mean expressions of PCK1 mRNA between patients with AdenoCas or CRPC-NE in the Beltran database. *$p < 0.05$ by a one-way ANOVA. **g, h** GSEAs of TCGA prostate dataset revealing significant correlations between higher PCK1 expression in prostate tissues with gene signatures representing PCa progression, p53 mutations, and RB1-knockdown (KD), neuronal development, CRPC-NE, and SCLC (**g**), and androgen-responsiveness (**h**). NES, normalised enrichment score; FDR, false discovery rate. **i** IF staining of ZBTB46 and PCK1 in a PCa TMA with antibodies for ZBTB46 (red) and PCK1 (green). Nuclei were visualised with DAPI staining (blue). Scale bars represent 20 µm. **j** Pearson's correlation analysis of PCK1 expression with LIF and ZBTB46 expressions in clinical tissue samples from the GSE21036 PCa dataset. $n = 111$. Data were tested by correlation XY analyses in GraphPad Prism.

to the GSEA in TCGA PCa database [20], PCa samples expressing high PCK1 levels also exhibited positive correlations with gene signatures involved in PCa progression (Wang [24], KEGG, and Sung [25]), p53 mutations [26], RB1-KD [27], neuronal development (GO and Reactome), CRPC-NE-responsive (Beltran [23] and Li [28]), and small-cell lung cancer (SCLC)-responsive (KEGG and Kim [29]) gene signatures (Fig. 5g). The GSEA also confirmed that patients with higher PCK1 levels exhibited negative correlations with gene signatures responsive to androgen signalling (Nelson [30], Wang [31], GO, and PID) (Fig. 5h). Significantly, co-immunofluorescent (co-IF) staining of the CRPC TMA confirmed that in high-grade prostate tumours, PCK1 expression was restricted to ZBTB46-positive tumour cells (Fig. 5i). Furthermore, the mean expression correlation was validated from the GSE21036 PCa dataset, which showed that PCK1 was positively correlated with LIF and ZBTB46 expressions according to a Pearson coefficient correlation analysis (Fig. 5j). These results supported the hypothesis that PCK1 overexpression is associated with ZBTB46 upregulation and is involved in the malignant progression and NE differentiation of PCa.

Targeting PCK1 reduces tumour growth of AR-negative and NE-like PCa cells

Inhibition of PCK1 is an effective treatment for CRC because it decreases glucose and glutamine utilisation, shifts cells toward anabolic metabolism, and reduces cell proliferation [12]. To assess the contribution of PCK1 to human PCa progression or its suppression, we stably introduced a PCK1 shRNA vector or a control vector into AR-negative PC3 and NE-like LASCPC01 cells. Significantly, PCK1-KD statistically reduced the growth rates of these cells in vitro (Fig. 6a). We further examined the functional relevance of the PCK1-mediated tumorsphere formation efficiency of the same two cell lines, and found that in three-dimensional growth assays in Matrigel, cells with PCK1-KD had reduced sphere formation, compared to cells that carried the control vector (Fig. 6b). Immunoblotting was used to validate PCK1 expression in cells with PCK1-KD (Fig. 6c). In order to test the pharmaceutical effect by targeting PCK1, we looked for PCK1 inhibitors, because we found two PCK inhibitors, 3-mercaptopropionic acid (3-MPA) [32] and a cPEPCK inhibitor [33], which are not approved for clinical use. We conducted in-house drug testing analysis as a screening platform to select candidate PCK1 inhibitors from a large number of compounds in an approved drug database [34]. Known PCK1 inhibitors were entered as a reference: 3-MPA [32] and cPEPCK inhibitor [33]. After selection, we identified two candidate PCK1 inhibitors respectively used to treat chronic myeloid leukaemia (CML) and metastatic breast cancer: nilotinib [35] and lapatinib [36]. Interestingly, our results revealed greater sensitivity of the AR-negative PC3 and NE-like LASCPC01 cell lines to nilotinib and lapatinib than to the cPEPCK inhibitor (Fig. 6d, e and Supplementary Fig. S2A). To test the drug sensitivity of PCK1-induced cells to nilotinib and lapatinib, AR-positive LNCaP cells overexpressing Tet-PCK1 were treated with increasing doses of nilotinib or lapatinib. We found that PCK1-inducing cells exhibited significantly reduced cell viability compared to cells in which PCK1 was not induced (Supplementary Fig. S2B, C). Moreover, PC3 and LASCPC01 cells treated with nilotinib and lapatinib showed strong decreases in PCK1 expression (Fig. 6f), supporting nilotinib and lapatinib being able to target PCK1 in PCa cells. Since we demonstrated that enzalutamide-resistant LNCaP-MDVR cells had higher PCK1 expression than parental LNCaP cells (Fig. 2A, B), a sphere formation assay confirmed that LNCaP-MDVR cells were significantly induced compared to parental LNCaP cells (Fig. 6g, h). However, when we used cPEPCK, nilotinib, and lapatinib to inhibit PCK1 expression in LNCaP-MDVR cells, cells treated with nilotinib and lapatinib formed fewer spheres compared to cells treated with cPEPCK (Fig. 6g, h). Consistently, treating PC3 and LASCPC01 cells with nilotinib and lapatinib produced robust reductions in sphere formation, while these cells were not sensitised to cPEPCK (Fig. 6i, j). These results were supported by further in vivo experiments. Mice were administered subcutaneous injections of PC3 and LASCPC01 cells and treated with nilotinib and lapatinib twice a week. Tumour-bearing mice treated with nilotinib and lapatinib exhibited dramatically decreased tumour formation (Fig. 6k, l) and tumour weights (Fig. 6m), compared to control mice. These results confirmed that targeting PCK1 by nilotinib and lapatinib can reduce the tumour growth efficiency of both AR-negative and NE-like PCa cells in vitro and in vivo. In summary, our study took advantage of the highly aggressive PCa or therapy-induced CRPC-NE to identify prognostic biomarkers and establish new therapeutic approaches for these diseases. In this study, we linked ADT-induced LIF/ZBTB46 signalling to PCK1-driven NE differentiation, and further explored its regulatory role in glucose metabolism (Fig. 6n).

DISCUSSION

PCK1 is one of the pivotal regulators in metabolic reprogramming [8], and we examined the detailed mechanism through which PCK1 regulates glucose metabolism-associated malignant progression and therapy-induced NE differentiation of PCa. Our results identified PCK1 as a potential therapeutic target for hormone therapy and explored the regulatory mechanisms by which LIF/ZBTB46 modulates PCK1 levels. Our study validated a canonical model in which the inactivation of AR signalling activates LIF/ZBTB46 signalling, leading to increase levels of PCK1 and NE markers and stimulating glucose metabolism and tumorigenesis of PCa. Activation of the LIF/ZBTB46 axis relieved the oncogenic effect of PCK1 on tumour growth and NE differentiation, resulting in a programme to develop CRPC-NE. Our study addressed the most urgent clinical issues and developed effective biosignatures and therapeutic strategies for the potentially effective detection and elimination of CRPC-NE.

Our results produced insights into PCK1 upregulation that leads to CRPC-NE progression and promotes glucose metabolism, depending on the physiological context after ADT. We addressed new diagnostic and prognostic information for current AR-directed therapeutic strategies by targeting changes in PCK1 expression occurring in response to ADT resistance. Since there is no approved clinical use of small molecules or gene-silencing agents targeting PCK1 [32, 33], we found two clinically used compounds (nilotinib and lapatinib) that targeted PCK1 and caused AR-negative and NE-like PCa death. Nilotinib was developed for targeting the BCR-ABI fusion protein and mutant platelet-derived growth factor receptor (PDGFR), and it is frequently applied in CML [35]. Lapatinib is a human epidermal growth factor receptor 2 (HER2) (ErbB2) inhibitor, and it is approved for breast cancer treatment [37]. We tested the effects of nilotinib and lapatinib by examining PCK1 levels in cells treated with these drugs, and found that AR-negative PC3 and NE-like LASCPC01 cells treated with nilotinib and lapatinib showed strong decreases in PCK1 expression. Moreover, we further tested the drug sensitivity of PCK1-induced cells to nilotinib and lapatinib, and found that AR-positive LNCaP cells with PCK1 overexpression had significantly reduced cell viability at increased doses of both nilotinib and lapatinib. Our study clearly emphasises that modulating the activity or expression of PCK1 may impact the growth of PCa cells.

Our results demonstrated that PCK1 had positive feedback activity of upregulating ZBTB46 expression. During PCa progression, the metabolic profile changes, in which gluconeogenesis, oxidative phosphorylation, and lipogenesis are upregulated [6]. Due to the essential role of AR signalling in controlling prostatic cell metabolism, upregulation of de novo lipogenesis is frequently observed in CRPC [38]. ADT was shown to induce the accumulation of external adipocyte differentiation-related proteins (AGRPs) and promote lipid accumulation [39]. That is, de novo lipogenesis might be a cause of activation of ADT-mediated drug resistance in PCa. In HCC, Xu et al. discovered that PCK1 is phosphorylated by AKT at serine 90, and this phosphorylation changes the cytological role of PCK1, thereby phosphorylating the insulin-induced gene 1/2 (INSIG-1/2), a repressor of SREBP, and ultimately activating lipogenesis [40]. This study provides evidence for the change in

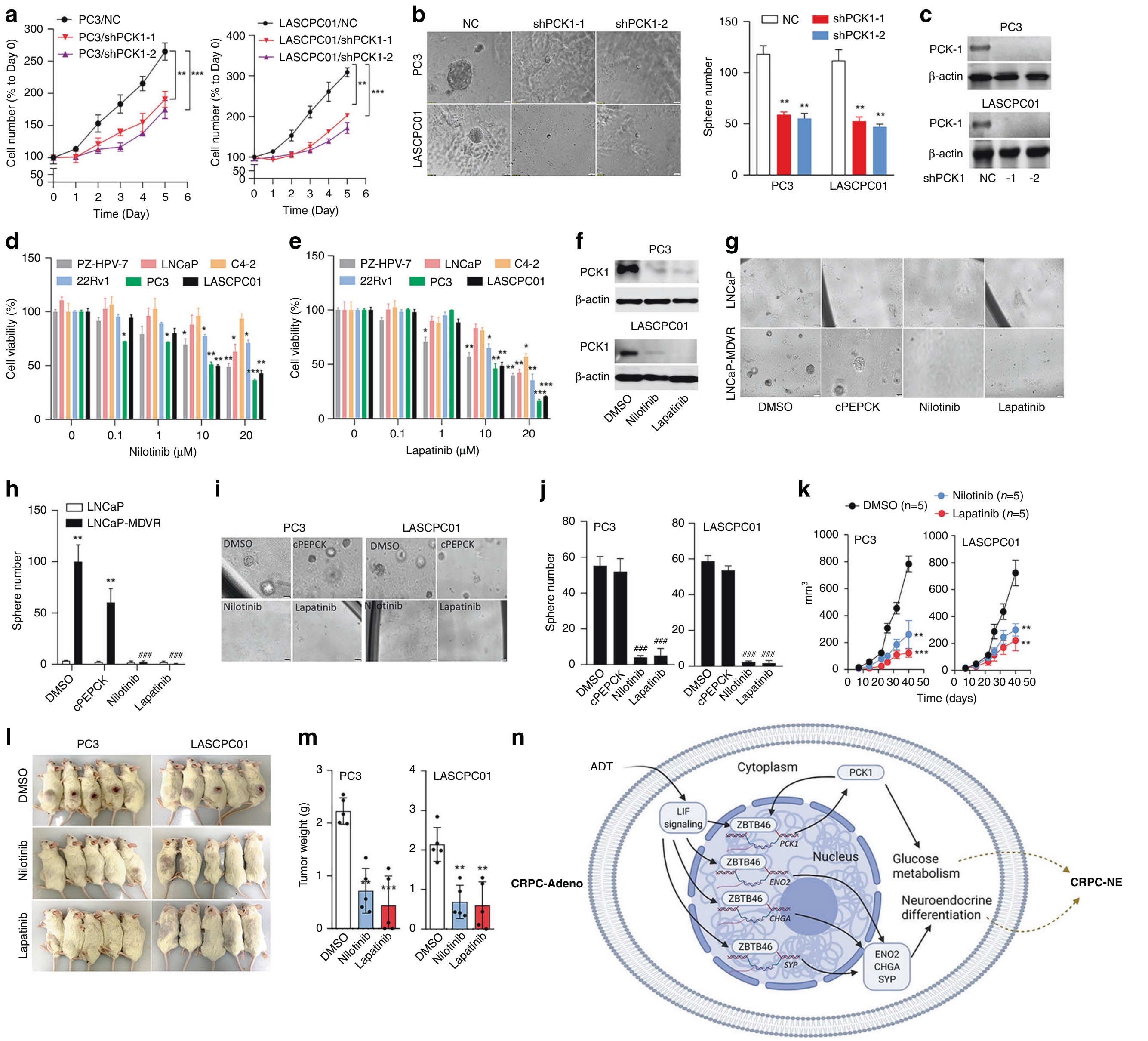

Fig. 6 Target PCK1 reduces tumour growth of AR-negative and ADT-resistant PCa cells. **a**, **b** Proliferation (**a**) and sphere formation (**b**) assays of PC3 and LASCPC01 cells expressing the non-target control (NC) or PCK1 shRNA. $n = 8$ per group. Values are expressed as the per cent change from cells transfected with NC shRNA. * vs. the NC. **$p < 0.01$ and ***$p < 0.001$ by a *t*-test. **c** Representative immunoblots of PCK1 protein levels in PC3 and LASCPC01 cells expressing the NC or PCK1 shRNA. **d**, **e** Various PCa cells were treated with 0, 0.1, 1, 10, and 20 μM nilotinib (**d**) or lapatinib (**e**), and cell viability was determined by an 3-(4,5-dimethylthiazol-2-yl)−2,5-diphenyltetrazolium bromide (MTT) colorimetric assay. * vs. the vehicle (0 μM). $n = 8$ per group. **f** Representative immunoblots of PCK1 protein levels in PC3 and LASCPC01 cells exposed to nilotinib (10 μM) or lapatinib (10 μM) for 1 week. **g**–**j** Sphere formation assays of parental LNCaP or MDV3100-resistant LNCaP-MDVR cells (**g**, **h**), and PC3 or LASCPC01 cells (**i**, **j**) exposed to cPEPCK (10 μM), nilotinib (10 μM), or lapatinib (10 μM) for 1 week. $n = 3$ per group. * vs. LNCaP; # vs. DMSO. **$p < 0.01$ and ***$p < 0.001$ by a *t*-test. Data from relative proliferation and sphere formation assays are the mean ± SEM of three independent experiments. **k**–**m** Tumour growth analysis of PC3 and LASCPC01 cells subcutaneously inoculated into male nude mice followed by treatment with nilotinib (25 mg/kg) or lapatinib (30 mg/kg) for 40 days. Tumour sizes were monitored once a week (**k**), and images (**l**) and tumour weights (**m**) were obtained at the end of the experiment ($n = 5$ mice per group). * vs. DMSO. *$p < 0.05$, **$p < 0.01$, and ***$p < 0.001$ by a *t*-test. **n** Summary of this study. ADT (black fade arrow) induces the activation of LIF signalling and increases the protein levels of a glucose metabolic enzyme, PCK1 and NE markers (CHGA, SYP, and ENO2) through enhancing the binding of ZBTB46 transcription factor to the regulatory sequences of *PCK1, CHGA, SYP*, and *ENO2*. Increased PCK1 altered glucose metabolism and reciprocally augmented ZBTB46 expression. The crosstalk between glucose metabolism and NE differentiation stimulates the trans-differentiation of CRPC-Adeno to CRPC-NE (green dot arrow).

the activity of PCK1 due to its phosphorylation. ADT may contribute to a lipid-rich environment in PCa cells, causing the phosphorylation of PCK1, and phosphorylated PCK1 may increase the modification of ZBTB46 and mediate its expression.

CRPC-NE is resistant to ADT and lacks a clinically effective chemotherapeutic choice [2]. The principal goal of this study was to identify prognostic biomarkers and establish new therapeutic targets for highly aggressive androgen-independent PCa and

CRPC-NE. In summary, this study reports on the molecular and therapeutic mechanisms of PCK1 which could lead to the further development of effective medications to eradicate currently incurable CRPC-NE. We linked PCK1 induced by ADT resistance to NE differentiation through LIF/ZBTB46-driven glucose metabolic signalling, and further explored its therapeutic effects on highly aggressive androgen-independent PCa and CRPC-NE. We demonstrated that strategies targeting PCK1 may be effective against PCa by modulating the PCK1-driven metabolic response, which in turn determines prostate malignancy and NE differentiation. We showed that PCK1 upregulation was strongly correlated with NE differentiation and a high therapeutic resistance potential by activating glucose metabolism in PCa.

DATA AVAILABILITY

The datasets used and/or analysed during the current study are available from the corresponding author on reasonable request.

REFERENCES

1. Dai C, Heemers H, Sharifi N. Androgen signaling in prostate cancer. Cold Spring Harb Perspect Med. 2017;7:a030452.
2. Patel GK, Chugh N, Tripathi M. Neuroendocrine differentiation of prostate cancer—an intriguing example of tumor evolution at play. Cancers. 2019; 11:1405.
3. Wang W, Epstein JI. Small cell carcinoma of the prostate. A morphologic and immunohistochemical study of 95 cases. Am J Surg Pathol. 2008;32:65–71.
4. Conteduca V, Oromendia C, Eng KW, Bareja R, Sigouros M, Molina A, et al. Clinical features of neuroendocrine prostate cancer. Eur J Cancer. 2019;121:7–18.
5. Aggarwal R, Huang J, Alumkal JJ, Zhang L, Feng FY, Thomas GV, et al. Clinical and genomic characterization of treatment-emergent small-cell neuroendocrine prostate cancer: a multi-institutional prospective study. J Clin Oncol. 2018;36:2492–503.
6. Tiwari R, Manzar N, Ateeq B. Dynamics of cellular plasticity in prostate cancer progression. Front Mol Biosci. 2020;7:130.
7. Liberti MV, Locasale JW. The Warburg effect: how does it benefit cancer cells? Trends Biochem Sci. 2016;41:211–8.
8. Wang Z, Dong C. Gluconeogenesis in cancer: function and regulation of PEPCK, FBPase, and G6Pase. Trends Cancer. 2019;5:30–45.
9. Latorre-Muro P, Baeza J, Armstrong EA, Hurtado-Guerrero R, Corzana F, Wu LE, et al. Dynamic acetylation of phosphoenolpyruvate carboxykinase toggles enzyme activity between gluconeogenic and anaplerotic reactions. Mol Cell. 2018;71:718–32. e719
10. Li Y, Zhang M, Dorfman RG, Pan Y, Tang D, Xu L, et al. SIRT2 promotes the migration and invasion of gastric cancer through RAS/ERK/JNK/MMP-9 pathway by increasing PEPCK1-related metabolism. Neoplasia. 2018;20:745–56.
11. Yamaguchi N, Weinberg EM, Nguyen A, Liberti MV, Goodarzi H, Janjigian YY, et al. PCK1 and DHODH drive colorectal cancer liver metastatic colonization and hypoxic growth by promoting nucleotide synthesis. Elife. 2019;8:e52135.
12. Montal ED, Bhalla K, Dewi RE, Ruiz CF, Haley JA, Ropell AE, et al. Inhibition of phosphoenolpyruvate carboxykinase blocks lactate utilization and impairs tumor growth in colorectal cancer. Cancer Metab. 2019;7:8.
13. Tuo L, Xiang J, Pan X, Gao Q, Zhang G, Yang Y, et al. PCK1 downregulation promotes TXNRD1 expression and hepatoma cell growth via the Nrf2/Keap1 pathway. Front Oncol. 2018;8:611.
14. Peng YB, Zhou J, Gao Y, Li YH, Wang H, Zhang M, et al. Normal prostate-derived stromal cells stimulate prostate cancer development. Cancer Sci. 2011;102:1630–5.
15. Faris JE, Smith MR. Metabolic sequelae associated with androgen deprivation therapy for prostate cancer. Curr Opin Endocrinol Diabetes Obes. 2010;17:240–6.
16. Liu YN, Niu S, Chen WY, Zhang Q, Tao Y, Chen WH, et al. Leukemia inhibitory factor promotes castration-resistant prostate cancer and neuroendocrine differentiation by activated ZBTB46. Clin Cancer Res. 2019;25:4128–40.
17. Gao B, Lue HW, Podolak J, Fan S, Zhang Y, Serawat A, et al. Multi-omics analyses detail metabolic reprogramming in lipids, carnitines, and use of glycolytic intermediates between prostate small cell neuroendocrine carcinoma and prostate adenocarcinoma. Metabolites. 2019;9:E82.
18. Lin SR, Wen YC, Yeh HL, Jiang KC, Chen WH, Mokgautsi N, et al. EGFR-upregulated LIFR promotes SUCLG2-dependent castration resistance and neuroendocrine differentiation of prostate cancer. Oncogene. 2020;39:6757–75.
19. Chen WY, Tsai YC, Siu MK, Yeh HL, Chen CL, Yin JJ, et al. Inhibition of the androgen receptor induces a novel tumor promoter, ZBTB46, for prostate cancer metastasis. Oncogene. 2017;36:6213–24.
20. Cancer Genome Atlas Research Network. The molecular taxonomy of primary prostate cancer. Cell. 2015;163:1011–25.
21. Meredith MM, Liu K, Kamphorst AO, Idoyaga J, Yamane A, Guermonprez P, et al. Zinc finger transcription factor zDC is a negative regulator required to prevent activation of classical dendritic cells in the steady state. J Exp Med. 2012;209:1583–93.
22. Taylor BS, Schultz N, Hieronymus H, Gopalan A, Xiao Y, Carver BS, et al. Integrative genomic profiling of human prostate cancer. Cancer Cell. 2010;18:11–22.
23. Beltran H, Prandi D, Mosquera JM, Benelli M, Puca L, Cyrta J, et al. Divergent clonal evolution of castration-resistant neuroendocrine prostate cancer. Nat Med. 2016;22:298–305.
24. Wang G, Wang J, Sadar MD. Crosstalk between the androgen receptor and beta-catenin in castrate-resistant prostate cancer. Cancer Res. 2008;68:9918–27.
25. Sung SY, Hsieh CL, Law A, Zhau HE, Pathak S, Multani AS, et al. Coevolution of prostate cancer and bone stroma in three-dimensional coculture: implications for cancer growth and metastasis. Cancer Res. 2008;68:9996–10003.
26. Elkon R, Rashi-Elkeles S, Lerenthal Y, Linhart C, Tenne T, Amariglio N, et al. Dissection of a DNA-damage-induced transcriptional network using a combination of microarrays, RNA interference and computational promoter analysis. Genome Biol. 2005;6:R43.
27. Chicas A, Wang X, Zhang C, McCurrach M, Zhao Z, Mert O, et al. Dissecting the unique role of the retinoblastoma tumor suppressor during cellular senescence. Cancer Cell. 2010;17:376–87.
28. Li, Y, He, Y, Butler, W, Xu, L, Chang, Y, Lei, K, et al. Targeting cellular heterogeneity with CXCR2 blockade for the treatment of therapy-resistant prostate cancer. Sci Transl Med. 2019;11:eaax0428.
29. Kim YH, Girard L, Giacomini CP, Wang P, Hernandez-Boussard T, Tibshirani R, et al. Combined microarray analysis of small cell lung cancer reveals altered apoptotic balance and distinct expression signatures of MYC family gene amplification. Oncogene. 2006;25:130–8.
30. Nelson PS, Clegg N, Arnold H, Ferguson C, Bonham M, White J, et al. The program of androgen-responsive genes in neoplastic prostate epithelium. Proc Natl Acad Sci USA. 2002;99:11890–5.
31. Wang G, Jones SJ, Marra MA, Sadar MD. Identification of genes targeted by the androgen and PKA signaling pathways in prostate cancer cells. Oncogene. 2006;25:7311–23.
32. Horton RW, Meldrum BS. Seizures induced by allylglycine, 3-mercaptopropionic acid and 4-deoxypyridoxine in mice and photosensitive baboons, and different modes of inhibition of cerebral glutamic acid decarboxylase. Br J Pharm. 1973;49:52–63.
33. Foley LH, Wang P, Dunten P, Ramsey G, Gubler ML, Wertheimer SJ. Modified 3-alkyl-1,8-dibenzylxanthines as GTP-competitive inhibitors of phosphoenolpyruvate carboxykinase. Bioorg Med Chem Lett. 2003;13:3607–10.
34. Meng XY, Zhang HX, Mezei M, Cui M. Molecular docking: a powerful approach for structure-based drug discovery. Curr Comput Aided Drug Des. 2011;7:146–57.
35. Blay J-Y, von Mehren M. Nilotinib: a novel, selective tyrosine kinase inhibitor. Semin Oncol. 2011;38:S3–S9.
36. Telli ML, Gradishar WJ, Ward JH. NCCN guidelines updates: breast cancer. J Natl Compr Canc Netw. 2019;17:552–5.
37. Scaltriti M, Verma C, Guzman M, Jimenez J, Parra JL, Pedersen K, et al. Lapatinib, a HER2 tyrosine kinase inhibitor, induces stabilization and accumulation of HER2 and potentiates trastuzumab-dependent cell cytotoxicity. Oncogene. 2008;28:803–14.
38. Lounis MA, Peant B, Leclerc-Desaulniers K, Ganguli D, Daneault C, Ruiz M, et al. Modulation of de novo lipogenesis improves response to enzalutamide treatment in prostate cancer. Cancers. 2020;12:3339.
39. Lin LC, Gao AC, Lai CH, Hsieh JT, Lin H. Induction of neuroendocrine differentiation in castration resistant prostate cancer cells by adipocyte differentiation-related protein (ADRP) delivered by exosomes. Cancer Lett. 2017;391:74–82.
40. Xu D, Wang Z, Xia Y, Shao F, Xia W, Wei Y, et al. The gluconeogenic enzyme PCK1 phosphorylates INSIG1/2 for lipogenesis. Nature. 2020;580:530–5.

ACKNOWLEDGEMENTS

We thank Dr Hsing-Jien Kung (Academician of the Academia Sinica, Chair Professor of Taipei Medical University) for reading the manuscript and providing comments and helpful suggestions. This work was jointly supported by grants from the Ministry of Science and Technology, Taiwan (MOST109-2326-B-038-001-MY3 and MOST110-2622-B-038-002 to Y-NL, and MOST109-2314-B-038-105 to Y-CW), the Taipei Medical University-Chi Mei Medical Center (110CM-TMU-07 to Y-NL), and the Higher Education Sprout Project by the Ministry of Education (MOE).

AUTHOR CONTRIBUTIONS
W-YC and Y-NL designed the experiments and supervised the project. Y-CW, C-LL, H-LY, W-HC, K-CJ, and VTNT performed the experiments. Y-CW, W-YC, and JH provided the human PCa samples. W-YC performed the histomorphometric analysis. H-LY constructed the databases and performed the statistical and computational analyses. MH provided assistance with animal experiments. Y-CW, C-LL, W-YC, and Y-NL wrote, reviewed, and/or revised the manuscript. All authors analysed and interpreted the data.

ETHICS APPROVAL AND CONSENT TO PARTICIPATE
CRPC and SCPC TMAs were obtained from Duke University School of Medicine, and their use was approved by the Duke University School of Medicine Institutional Review Board (protocol ID: Pro00070193). PCa tissue samples before and after ADT were collected from Taipei Medicine University-Wan-Fang Hospital (Taipei, Taiwan), the collection of which followed the Declaration of Helsinki and was approved by the Taipei Medical University Joint Institutional Review Board (protocol ID: N202103136). Protocols of in vivo experiment was followed "Guideline for the Care and Use of Laboratory Animals" published by Council of Agriculture and approved by Taipei Medical University Institutional Animal Care and Use Committee (approval ID LAC-2021-0111).

CONSENT FOR PUBLICATION
Not applicable.

COMPETING INTERESTS
The authors declare no competing interests.

ADDITIONAL INFORMATION
Supplementary information The online version contains supplementary material available at https://doi.org/10.1038/s41416-021-01631-3.

Correspondence and requests for materials should be addressed to Wei-Yu Chen or Yen-Nien Liu.

Reprints and permission information is available at http://www.nature.com/reprints

Publisher's note Springer Nature remains neutral with regard to jurisdictional claims in published maps and institutional affiliations.